Al^{3+} Coordination in Cryolitic Melts: A Computer Simulation Study

Michael J. Castiglione, Mauro C. C. Ribeiro, Mark Wilson, and Paul A. Madden
Physical and Theoretical Chemistry Laboratory, Oxford University,
South Parks Road, Oxford OX1 3QZ, U.K.
Reprint requests to Prof. P. A. M.; e-mail: madden@physchem.ox.ac.uk

Z. Naturforsch. **54 a,** 605–610 (1999); received August 23, 1999

The structures of melts containing cryolite have proved difficult to confirm, despite decades of study, on account of the high temperatures and corrosiveness of these melts. Raman spectroscopy has so far provided the majority of the insight into the aluminium coordination environments, but some of its interpretations are still debated.

In this paper we present the results of MD simulations on various NaF-AlF_3 liquid mixtures using published potentials developed for the solid state and published Raman spectra.

Key words: Cryolite; Raman Spectra; MD Simulation; Complex Ions.

1. Introduction

Gilbert and co-workers [1, 2] have proposed that, in melts of 1:1 NaF:AlF_3 mixtures, the only significant aluminium-containing species is the tetrahedral AlF_4^- ion. Despite the fact that only in a few compounds with large organic cations [3] solid state structures containing such ions have been confirmed, this four-coordination of aluminium is generally accepted to be present in $NaAlF_4$ melts. The most direct evidence for this is the four line Raman spectrum with the polarization characteristics expected for a tetrahedral molecule. The strong polarised band occurs at a frequency of 622 cm^{-1}, essentially the same as the symmetric stretching frequency observed for the $NaAlF_4$ gaseous molecule [4].

The continued presence of the 622 cm^{-1} band at lower AlF_3 mole fractions, together with a band at 560 cm^{-1} and a shoulder at 510 cm^{-1} in the polarised Raman spectrum is taken to mean that three aluminium-containing species are present in the Na_3AlF_6 melt (cryolite). Despite the fact that the polarised band in the solid cryolite (which contains *only* octahedrally coordinated aluminium) Raman spectrum is at 560 cm^{-1} [5], Gilbert assigns the liquid 560 cm^{-1} band to AlF_5^{2-}, and the 510 cm^{-1} band to AlF_6^{3-} because of the way the relative intensity of these features changes with composition. This assignment suggests that 5-coordinate aluminium is by far the dominant environment in liquid Na_3AlF_6. It is contested by other experimentalists [6], who question the existence of the 510 cm^{-1} shoulder, and prefer to assign the 560 cm^{-1} band to AlF_6^{3-} in the liquid as in the solid.

It is not generally thought that fluoride bridging between aluminium centres is significant [1] in the melts, despite its prevalence in solid state NaF-AlF_3 compounds with less than six fluorides per aluminium. The evidence for this is that thermodynamic measurements can be interpreted without the introduction of bridged species [7]. Furthermore, the viscosity is maximum at the cryolite (Na_3AlF_6) composition [8], whereas, if increased network formation occurred at lower NaF mole fraction, one would expect that the viscosity should increase.

2. Simulation of NaF:AlF_3 Melts

2.1. NaF:AlF_3 Mixtures

A potential [9] has been devised for NaF/AlF_3 mixtures which reproduces the known crystal structures of compounds of stoichiometry AlF_3, $NaAlF_4$, $Na_5Al_3F_{14}$ (chiolite) and Na_3AlF_6 as well as the structures of a number of gas-phase species which had been calculated by *ab initio* methods. These crystal structures are non-trivial, and polarization effects are found to play an important role in stabilizing them. The potentials have been used to study the vibrational frequencies of the isolated $MAlF_4$ molecules (M = alkali) and also of the solid compounds [10]. The vibrational spectra are in good accord with experimental

0932–0784 / 99 / 1000–0605 $ 06.00 © Verlag der Zeitschrift für Naturforschung, Tübingen · www.znaturforsch.com

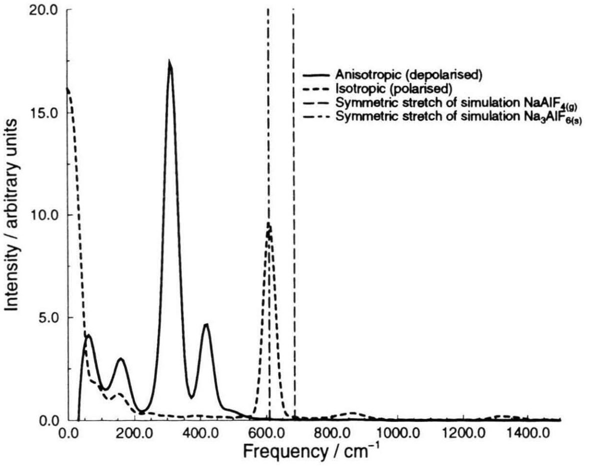

Fig. 1. Calculated Raman spectrum of solid cryolite at 300 K.

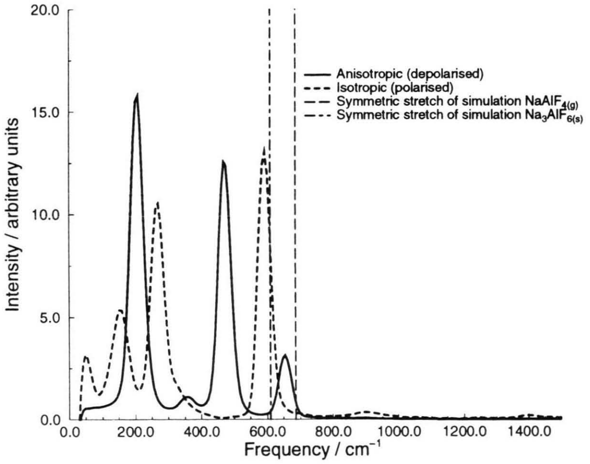

Fig. 2. Calculated Raman spectrum of solid chiolite at 300 K.

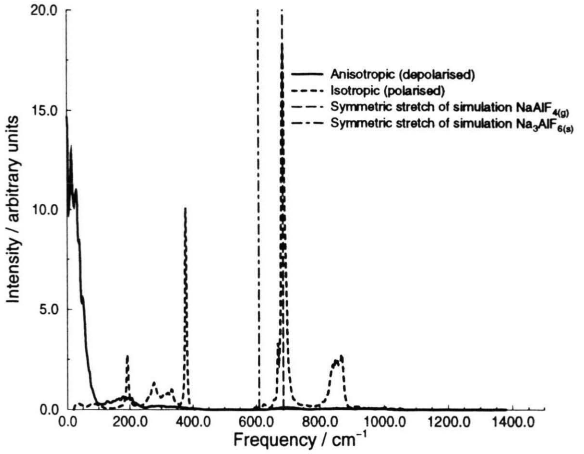

Fig. 3. Calculated Raman spectrum of the $NaAlF_4$ molecule at 1000 K.

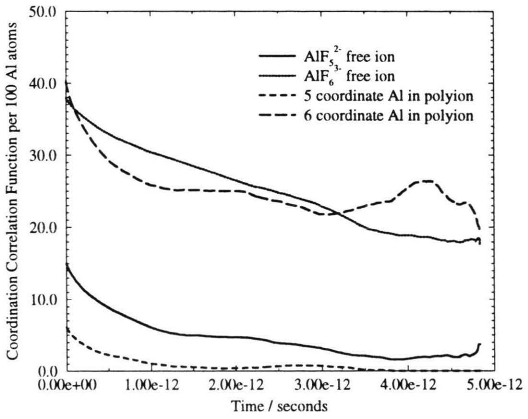

Fig. 4. Coordination number correlation functions in simulated liquid cryolite at 1300 K.

spectra [4] in both cases, though the calculated frequencies for the stretching of Al-F bonds are higher than those found experimentally. In particular the symmetric stretch peaks were by approximately 10% higher in frequency than experimentally (we attribute this to the use of an incompressible model [10, 11] for the F^- ion). Thus the experimental 622 cm^{-1} peak of the $NaAlF_4$ gas phase molecule appeared at 700 cm^{-1} in the simulation, Fig. 3, and the 560 cm^{-1} band of the cryolite crystal appeared at 620 cm^{-1} in the simulation. Raman spectra for the cryolite and chiolite crystals and for the $NaAlF_4$ molecule, calculated with the polarizability model described below, are shown in Figures 1 - 3. In these figures we show by vertical lines the positions of the calculated polarised lines in solid cryolite and gas-phase $NaAlF_4$. These serve as reference frequencies for the calculated Raman spectra.

This potential has now been used in simulations of the melts over a range of compositions from Na_3AlF_6 to $NaAlF_4$. The calculations were carried out at temperatures close to the experimental melting point, ~ 1300 K, and at the corresponding densities, as tabulated in [12]. Coordination number correlation functions were calculated for all melts and are given, for Na_3AlF_6, in Figure 4.

The $t = 0$ value of these functions gives the average number percentage of Al^{3+} ions found with

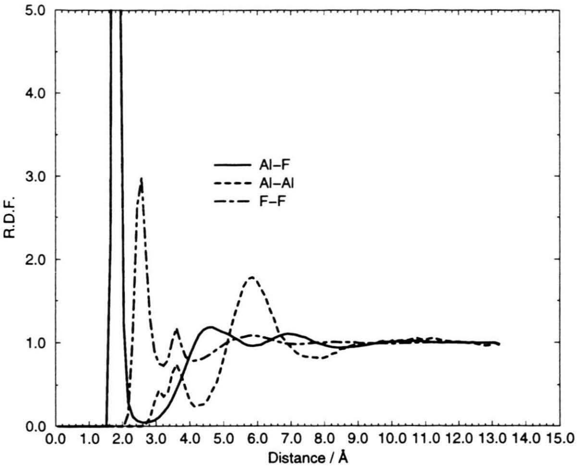

Fig. 5. Radial distribution functions of simulated liquid cryolite at 1300 K.

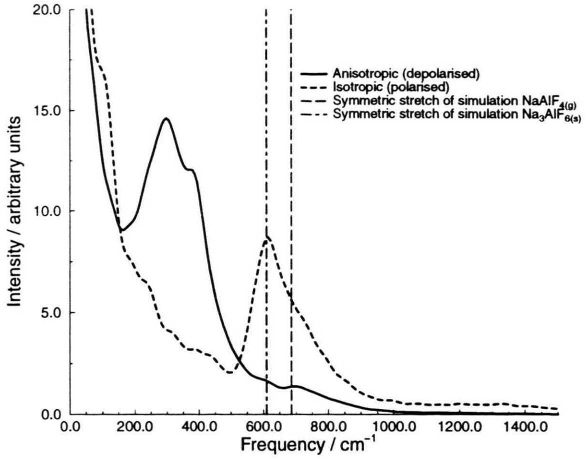

Fig. 6. Calculated Raman spectrum of Na_3AlF_6 liquid at 1300 K.

that coordination number in the melt, and the rate of decay of the function with time indicates the lifetime. These coordination number correlation functions clearly show that 6-coordination dominates all simulated NaF-AlF_3 mixtures, with an increasing importance of 5-coordination and polymerisation of AlF_n units as the NaF mole fraction decreases, and thus the number of fluorides available to coordinate to aluminium diminishes. This is in contrast to the existing models of dissociation for cryolitic liquids [1], which suggest purely a partial dissociation of $AlF_6{}^{3-}$ to form either $AlF_5{}^{2-}$ and $AlF_4{}^{-}$ or $AlF_4{}^{-}$ only. In the simulations almost no $AlF_4{}^{-}$ is observed, even for the $NaAlF_4$ melt.

Radial distribution functions (RDF) for the various melts, shown for Na_3AlF_6 in Fig. 5, all show a peak in the 3.5 Å region of the Al-Al partial RDF, and this increases as the AlF_3 mole fraction increases. This peak (actually composed of two overlapping peaks) occurs at too short a distance to be due to a 'van der Waals' interaction between two AlF_n complex ions, and must be an Al-F-Al linkage. The inner peak corresponds to an edge-shared unit, whilst the outer peak corresponds to a vertex-shared linkage.

2.2. *Simulated Raman Spectra of NaF:AlF$_3$ Mixtures*

Since the primary experimental evidence for the two- or three-species models is Raman spectroscopy, we have calculated Raman spectra for the simulated liquids by adopting a particular model for the dependence of the melt polarizability on the ionic coordinates. Formulation of such a model is a difficult task and has been discussed for somewhat simpler melts, binary alkali halides, in previous work [13 - 15]. For a melt of the complexity of NaF/AlF_3 it is not presently possible to obtain a quantitative polarizability model. Hence, in the present work, we simply adopt a single component of the alkali halide work, the so-called γ hyperpolarizability mechanism, as a representative and physically-motivated model for the dependence of the polarizability on the ionic coordinates. The consequence of using a different model for the polarizability would be that, although the band positions would be conserved (as a property of the underlying interaction potential) the relative intensities and degrees of polarisation of different bands may change substantially. The γ hyperpolarizability mechanism was found to reproduce quite well the relative intensities of different bands observed for the isolated $MAlF_4$ molecules and for the crystals. We obtain the spectra for the melt from [14]

$$I_{ab}^{\mathrm{MD}}(\omega) = \int_0^\infty \mathrm{d}t\, e^{i\omega t} \langle \Pi_{ab}(t) \Pi_{ab}(0) \rangle. \qquad (1)$$

Here, $I_{ab}^{\mathrm{MD}}(\omega)$ is the spectrum calculated for polarization ab at frequency ω, and $\Pi_{ab}(t)$ is the value of the ab^{th} cartesian component of the polarizability of the melt evaluated with the ionic coordinates at time t.

Despite the contrast between our observations about the melt structures and the accepted two- or three-species model, we find considerable accord

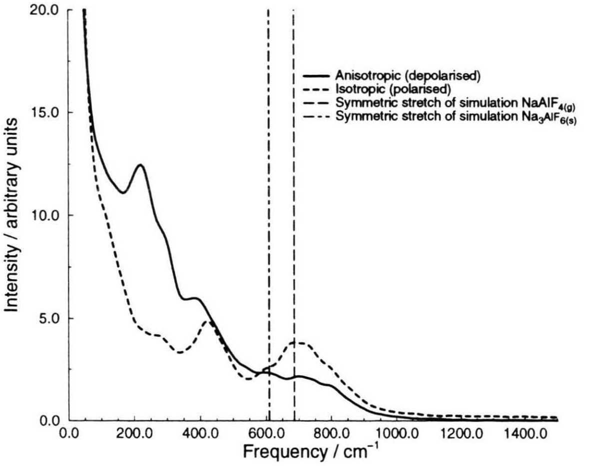

Fig. 7. Calculated Raman spectrum of $NaAlF_4$ liquid at 1300 K.

between our results and the experimental Raman observations. As shown in Fig. 6, the liquid Na_3AlF_6 simulation gave a calculated Raman spectrum very similar to that observed experimentally: the isotropic part contains a peak at 620 cm^{-1} with a clear shoulder at 700 cm^{-1}, and the anisotropic part has a single peak at 350 cm^{-1} (experimental 320 cm^{-1}). Thus, just as observed experimentally, the simulation spectrum contained a depolarised band at around 350 cm^{-1}, and a main polarised band at a position corresponding *exactly to that observed in solid cryolite* with a shoulder corresponding *exactly to the position of the polarized band observed in gaseous* $NaAlF_4$.

At first sight, the spectrum for the $NaAlF_4$ simulation, Fig. 7, is also similar to the experimental observation. There is a strong, polarized band at the same position ~ 700 cm^{-1} as that calculated for the $NaAlF_4$ molecule; this corresponds to the 622 cm^{-1} band observed experimentally and assigned to the AlF_4^- ion. Note that this shift in the position of the polarized high frequency band from Na_3AlF_6 to $NaAlF_4$ occurs despite the fact that no significant change in coordination number is seen in the simulations. There are also weaker bands at 220 cm^{-1} and 420 cm^{-1}, with a possible weak band at ca. 800 cm^{-1}, corresponding perhaps to the experimental bands at 215, 320, and 760 cm^{-1}. However, on closer examination, it can be seen that the polarization characteristics of these bands do not accord well with experiment. The high frequency band is *very* strongly polarized in the experimental spectrum (consistent with the interpretation as the symmetric stretch of a tetrahedron) but, as the figure shows, there is appreciable intensity in the simulated anisotropic spectrum at this frequency. Also, the 420 cm^{-1} band shows appreciable intensity in the isotropic part of the spectrum. This is in contradiction to experiment, where this band is depolarized. As we have remarked, the relative intensity of different features is affected by the details of the (somewhat arbitrarily chosen) polarization model, but the high degree of polarization of the experimental bands does seem indicative of a highly symmetrical underlying structure which would be reflected by the polarizability model if it were true of the ionic structure in the simulation. This gives a first indication that, at this composition, the simulation did not reproduce the true structure perfectly.

The Na_2AlF_5 spectrum is intermediate between the Na_3AlF_6 and $NaAlF_4$ spectra (as it is experimentally [1]), with bands common to both spectra appearing with appropriate changes of intensity. In particular, the 700 cm^{-1} feature which appears as a weak high frequency shoulder on the main 620 cm^{-1} band in Na_3AlF_6 has become more pronounced and distinctive in Na_2AlF_5.

The simulated melt spectra then *appear* to be consistent with a picture of a liquid composed of at least two species (to be associated with the 620 cm^{-1} and 700 cm^{-1} bands) whose proportion shifts with changing composition of the melt. However, the analysis of the local coordination environment of the Al^{3+} shows that these ions are predominantly six-coordinate at all the compositions studied and does not support the identification of these two bands with differently coordinate Al^{3+} centres.

2.3. Na_3AlF_6:NaCl Melts

The complexity of the simulated spectra must be associated with the network structure associated with the linking of the six-coordinate sites. By adding a 'network-breaker' to the system, we might hope to disrupt the network linkages and produce the isolated molecular ions conventionally assumed to occur in the pure melts. Brooker [6] has obtained Raman spectra of a solution of Na_3AlF_6 in liquid CsCl at 1023 K, which show two polarised bands, these being the familiar (approximately) 560 and 620 cm^{-1}, as observed in the Raman spectrum of pure molten cryolite, although in this dilute (10%) solution, the two bands are quite distinct. Brooker claims that there is no shoulder at 510 cm^{-1}, assigning the peaks to

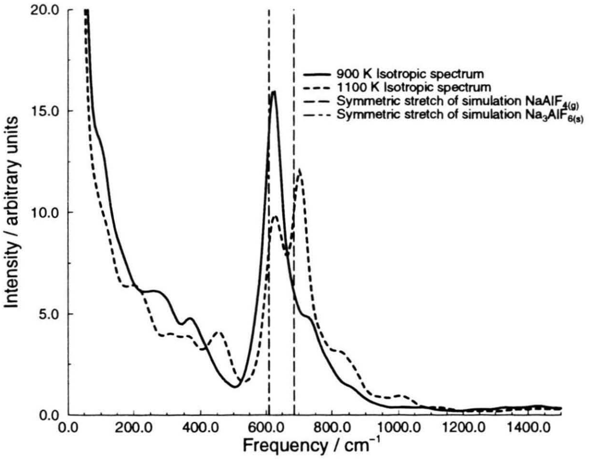

Fig. 8. Calculated Raman spectrum of 10% Na_3AlF_6 in NaCl.

$AlF_6{}^{3-}$ and $AlF_4{}^{-}$ respectively. We have performed simulations of an analogous system, although instead of using CsCl as the solvent, in order to keep the simulations as simple as possible, we used NaCl. To save computational time the chloride ions are assumed to be non-polarisable. Whilst at first this may seem a poor approximation, when we have already stressed the importance of fluoride polarisation in AlF_3-containing systems [9], it is believed [6] that when Na_3AlF_6 is dissolved in NaCl, no chloride enters the aluminium's first coordination sphere. Hence the only nearest-neighbour interactions between Cl^- and a cation will involve Na^+ as the cation, and since Na^+ is not a very polarising cation, the polarisation of chloride will be small.

For such a solution we find good qualitative agreement with experiment, in that the 620 and 700 cm^{-1} bands in the simulated isotropic spectrum are distinct (Figure 8).

Not only this, but the expected temperature variation in the isotropic spectrum was qualitatively reproduced: at 900 K the 700 cm^{-1} band was just a shoulder, whereas at 1100 K the 700 cm^{-1} band was more intense than the 620 cm^{-1} band.

Coordination number analysis for the melt confirms that network breakdown has occurred, with no Al-F-Al linkages remaining. Furthermore, no Cl^- ions are found in the first coordination shell. Analysis of the Al^{3+} coordination shows that at 900 K it is approximately 59% $AlF_5{}^{2-}$ and 41% $AlF_6{}^{3-}$ whilst at 1100 K, approximately 6% $AlF_4{}^{-}$, 64% $AlF_5{}^{2-}$ and 44% $AlF_6{}^{3-}$. This clearly shows the decrease in average coordination number expected with a rise in temperature. Furthermore, the results confirm that the simulation model *is* capable of producing an equilibrium between the 4-, 5- and 6-coordinate Al^{3+} centres. At 1100 K the coordination number distribution is fairly similar to the Gilbert model for pure liquid cryolite. More generally, they show that 5-coordination is not an unrealistic proposition (at least in a melt), as has been argued on electrostatic grounds.

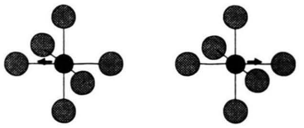

Fig. 9. Symmetric motion of aluminium ions within a melt, as postulated to explain the high frequency band in calculated spectra.

However, the problem of assigning the two Raman bands remains, when clearly there are three species present. To address this we use Instantaneous Normal Mode (INM) analysis [16, 17], which consists of calculating the vibrational normal modes at several instantaneous configurations along the MD run. The analysis of these modes is a realistic proposition for these systems in which there are only five aluminium ions, and we wish to consider only Al^{3+} and F^- ions, but this is quite impossible for the pure cryolite simulations in which there are 32 Al^{3+} and 192 F^- ions per simulation cell.

INM analysis does not show a correlation between the coordination number of the aluminium and the vibration frequency of the species. Vibrations of 5- and 6-coordinate aluminium span the range of frequencies observed in the calculated isotropic Raman spectrum, rather than conforming to an ordering of vibrational frequencies $\nu_{AlF_6^{3-}} < \nu_{AlF_5^{2-}} < \nu_{AlF_4^-}$. To investigate further, a configuration involving only $AlF_6{}^{3-}$ ions within the solution was generated and allowed to undergo thermal motion for several picoseconds. INM analysis was then performed. In this case the results were more conclusive: symmetric stretches of the $AlF_6{}^{3-}$ ions occurred in the range of the 620 cm^{-1} band, whilst symmetric motions of nearby aluminium ions of the type shown in Fig. 9 occurred in the range of the 700 cm^{-1}.

This leads us to believe that, of the two main peaks in the 500 - 700 cm^{-1} region (experimentally 560 and 622 cm^{-1}, simulation 620 and 700 cm^{-1}), the lower frequency peak is due largely to symmetric stretches of isolated $AlF_n{}^{(n-3)-}$ polyhedra, just as in solid cryolite, and the higher frequency peak is a result of symmetric motions of nearby Al^{3+} ions, whether directly bonded via a fluoride or not. This is certainly true for a simulation of 10% cryolite in NaCl in which all aluminium ions are set up to be six-coordinate, and one could deduce that, as the number of Al-F-Al linkages increases, as it does in simulations of NaF:AlF_3 mixtures as the mole fraction of NaF declines, the intensity of the peak due to coupling of motions between nearby aluminium centres would increase, leading ultimately to a situation in which this was the only feature in the high frequency part of the isotropic spectrum, as observed for liquid $NaAlF_4$.

3. Conclusion

We have obtained spectra that are similar to those obtained experimentally for quite a broad range of AlF_3/NaF compositions, despite a very different liquid structure to that deduced from the experimental spectra. In particular, we observe strong isotropic bands at the positions of the octahedral stretch of solid cryolite, and at the position of the tetrahedral stretch of the isolated $NaAlF_4$ molecule, and the relative intensities of these bands shift with composition as in the experimental spectra. Why one observes a band in the simulated liquid at a frequency corresponding to that of an AlF_4 tetrahedron in the gas phase, when there are almost no 4-coordinate Al^{3+} centres, has not been completely resolved. The appearance of the high frequency band in the simulation appears to be caused by vibrations involving Al^{3+} centres in close proximity. As the NaF concentration is reduced, such close approaches are induced by F^- bridging between 6-coordinate centres. The composition dependence of the intensities is therefore not associated with a change in coordination number. The simulation thus points to a scenario in which well-resolved bands may appear, whose intensities shift with composition, but which are not associated with distinct coordination centres.

Although for the simulated spectra there is no link between these bands and particular $AlF_n^{(n-3)-}$ ions, it does not follow that this is the case for *real* cryolitic melts. Although the simulated spectra resemble the experimental ones, there are significant discrepancies. This is particularly true for the $NaAlF_4$ composition, where the polarization of the bands is very different from that observed experimentally. Although this *might* be due to the simplistic polarizability model assumed in the calculations, the experimental spectra are very suggestive of scattering from tetrahedral molecular ion units. Furthermore, the bulk properties (*e.g.* viscosity) do not vary with composition as one would expect if there was an increasing degree of network formation for low NaF concentrations. The potential model produces an excellent account of the crystalline phases of NaF/AlF_3 mixtures, and does sustain an equilibrium between differently coordinated Al^{3+} centres, as indicated by the NaF/AlF_3/NaCl results but, on the balance of the available evidence, does seem to overstabilize the 6-coordinate species and hence favour network formation to a change in coordination number at low F^- activity.

Acknowledgements

The work was supported by EPSRC grant GR/L/49369. M.W. is grateful to the Royal Society for the award of a Research Fellowship.

[1] B. Gilbert, E. Robert, E. Tixhon, J. Olsen, and T. Østvold, Inorg. Chem. **35**, 4198 (1996).
[2] B. Gilbert and T. Materne, Applied Spectrocopy **44, 2** (1990).
[3] N. Herron, D. L. Thorn, R. L. Harlow, and F. Davidson, J. Amer. Chem. Soc. **115**, 3028 (1993).
[4] G. N. Papatheodorou, Current Topics in Materials Science **10**, 249 (1982).
[5] M. H. Brooker, Proceedings from the International Harald A. Øye Symposium, M. Sørlie, T. Østvold, and R. Huglen (Eds.), 1995.
[6] M. H. Brooker, private communication.
[7] E. W. Dewing, Proceedings of the Fifth International Symposium on Molten Salts, M .L. Saboungi, D. S. Newman, K. Johnson, and D. Inman (Eds.), The Electrochemical Society Proceedings 86; The Electrochemical Society, New York 1986.
[8] V. Danek, private communication.
[9] M. J. Castiglione, M. Wilson and P. A. Madden, Physical Chemistry Chemical Physics **1**, 165 (1999).
[10] M. J. Castiglione, M. C. C. Ribeiro, M. Wilson and P. A. Madden, to be published.
[11] A. J. Rowley, P. Jemmer, M. Wilson, and P. A. Madden, J. Chem. Phys. **108**, 10209 (1998).
[12] G. J. Janz and R. P. T. Tomkins, J. Phys. Chem. Ref. Data, **12-3**, 659 (1983).
[13] P. A. Madden and J. Board, JCS Faraday Trans II **83**, 1891 (1987).
[14] P. A. Madden, J. Board, K. O'Sullivan, and P. W. Fowler, J. Chem. Phys, **94**, 918 (1991).
[15] K. F. O'Sullivan and P. A. Madden, J. Phys. Condens. Matt. **3**, 8751 (1991).
[16] R. M. Stratt, Acc. Chem. Res. **28**, 201 (1995).
[17] T. Keyes, J. Phys. Chem. **101**, 2921 (1997).